JOURNAL OF GEOPHYSICAL RESEARCH, VOL. 101, NO. A3, PAGES 5381–5389, MARCH 1, 1996

VLF remote sensing of the auroral electrojet

S. A. Cummer, T. F. Bell, and U. S. Inan

Space, Telecommunications and Radioscience Laboratory, Stanford University, Stanford, California

L. J. Zanetti

Applied Physics Laboratory, Johns Hopkins University, Laurel, Maryland

Abstract. We investigate a new potential technique to determine the position of the auroral electrojet from ground-based VLF amplitude and phase measurements. The chief advantage of this technique over conventional ground magnetometer measurements is that it can provide data on a continental scale with a small number of receiving stations and with a minimum of data processing. At the edge of the auroral zone, where the electrojet current system flows, high-energy ($E > 300$ keV) precipitating electrons cause local electron density enhancements in the ionosphere which cause phase and amplitude perturbations in VLF waves propagating in the Earth-ionosphere waveguide. Continuous measurements of the amplitude and phase of signals from the Omega North Dakota VLF transmitter were made in Nome, Alaska. Using a two-dimensional model of VLF propagation which accounts for ionospheric disturbances caused by the electron precipitation associated with the electrojet, the amplitude and phase signatures of electrojet incursion across each propagation path were predicted. Seventeen nights of simultaneous VLF amplitude and phase data and ground magnetometer data were examined and catalogued based on the degree of temporal correlation between the two data sets and the degree to which the VLF events matched the propagation simulations. Of the nights exhibiting activity, more than 60% exhibited excellent correlation between the magnetometer and VLF events, and the majority of these showed good agreement with the model results. An additional estimate of the electrojet position was provided for one of the studied nights by field-aligned current measurements from the Freja satellite. A comparison of these independent means of determining the electrojet position shows that they are in good agreement for the night examined.

1. Introduction

The measurement of the position and intensity of the auroral electrojet is important in understanding a number of significant aspects of ionosphere-magnetosphere coupling. The high-energy particle precipitation that usually accompanies the electrojet [*Kikuchi and Evans*, 1983] is a major source of energy input into the lower ionosphere [*Chenette et al.*, 1993] and can cause substantial changes in the chemistry of this region [*Callis et al.*, 1991; *Baker et al.*, 1993]. Additionally, it is believed that Joule heating associated with sudden increases in the auroral electrojet current may be responsible for the generation of atmospheric gravity waves [*Yeh and Liu*, 1974; *Francis*, 1974; *Hunsucker*, 1982]. Continuous and real-time electrojet measurements could also help to avoid disruptions of electric power systems caused by geomagnetically induced currents (GICs) [*Ringlee*, 1989], as occurred, for example, during an intense geomagnetic storm on March 13, 1989.

Conventionally, the location and intensity of the auroral electrojet are determined from measurements of local magnetic field perturbations, which are assumed to be caused by horizontal ionospheric currents. However, magnetometers are only single-point measurement systems, and a continental-scale estimate of the auroral electrojet position based on these observations requires data from many stations and considerable analysis [*Kamide et al.*, 1982].

A satellite-based technique of determining the electrojet location involves the measurement of geomagnetic field-aligned (Birkeland) currents. It has been found that the equatorward boundary of the region 2 currents is at the same magnetic latitude as the auroral electrojet [*Zanetti et al.*, 1983]. From satellite magnetometer measurements one can detect the boundary of the field-aligned current regions and thus infer the position of the low-latitude boundary of the auroral electrojet. As this is a space-based measurement, however, it is difficult to provide continuous monitoring of a specific area.

Paper number 95JA03409.
0148-0227/96/95JA-03409$02.00

The measurement of characteristic perturbations in the phase and amplitude of subionospherically propagating VLF signals has been employed as a powerful tool for remote sensing of localized disturbances of the lower ionosphere [e.g., *Inan et al.*, 1990; *Burgess and Inan*, 1993]. *Potemra and Rosenberg* [1973] used VLF phase measurements to study midlatitude ionospheric disturbances caused by electron precipitation associated with geomagnetic storms. *Kikuchi and Evans* [1983] found, from a combination of ground-based VLF phase measurements, ground magnetometer observations, and satellite particle precipitation data, that the precipitation of $E > 300$ keV electrons in the auroral zone causes VLF phase anomalies which are completely correlated in time with auroral electrojet expansions.

These high-energy precipitating electrons penetrate to altitudes as low as 60 km where they can generate secondary ionization and affect the propagation of VLF waves in the Earth-ionosphere waveguide. Hence, as the auroral electrojet crosses a VLF great-circle propagation path, the amplitude and phase of the signal at the receiving station exhibit variations caused by this electron precipitation. Figure 1 shows a schematic description of this process.

The VLF technique would have significant advantages compared to these other methods. Continuous nighttime coverage over the entire northern United States and Canada could be obtained with a few well-placed receiving stations, compared to the tens of ground magnetometer stations required for similar coverage. Estimates of electrojet position using the VLF technique could even be obtained over the Atlantic Ocean, where placement of ground magnetometers is not feasible. These differences are due to the fact that VLF measurements can give information as to whether the electrojet has crossed a line (or propagation path), while magnetometer stations yield whether the electrojet has passed over a single point.

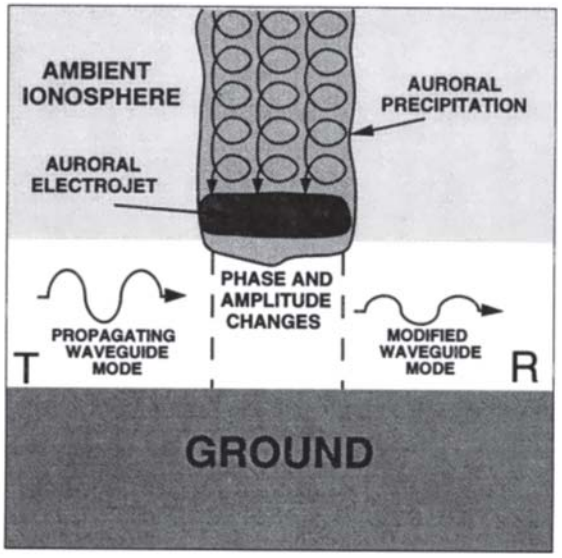

Figure 1. Interaction between the auroral electrojet and VLF waves. A transmitter (T) launches a VLF signal into the Earth-ionosphere waveguide. The waveguide signal propagating under the region of the electrojet incursion is modified due to the conductivity changes in the ionosphere caused by the $E > 300$ keV electron precipitation associated with the electrojet. The penetration of the electrojet over the propagation path is observed at the receiver (R) as phase and amplitude variations in the VLF signal.

To illustrate the main features of this new potential technique, we present results from the analysis of 17 nights (January 4-6 and 23-31, 1993; February 23-26 and 28, 1993) of simultaneous VLF propagation data from a single path and ground magnetometer observations. We find that of the nights showing geomagnetic activity over the region of interest, more than 60% show a strong temporal correlation between the onset of magnetic and VLF signatures seen in both the phase and amplitude data. Additionally, on most of the well-correlated nights, the form and magnitude of the observed VLF signatures are well-predicted by those simulated using a two-dimensional VLF propagation model [*Ferguson and Snyder*, 1987].

2. Details of the Study

Narrow-band observations of the signal from the Omega North Dakota VLF transmitter were made in Nome, Alaska in early 1993. Figure 2 shows the geographic configuration of this great circle propagation path. This configuration was chosen so that during geomagnetically quiet times, the auroral electrojet would likely lie north of all the great circle paths, but as activity increased, the currents would move southward and cross the paths, altering the Earth-ionosphere waveguide and perturbing the VLF waves propagating therein.

Magnetometer data over the same time period from the College, Alaska (CMO) and Fort Simpson, Northwest Territories (FSP) stations (see Figure 2) were also examined for evidence of the auroral electrojet. These stations are critically located near the point of highest geomagnetic latitude on the VLF propagation paths, which is where we expect the electrojet to initially cross the VLF paths. We expect the onset of magnetometer and VLF electrojet signatures to occur nearly simultaneously for this particular configuration.

In order to predict the nature of the VLF amplitude and phase signatures caused by the presence of the auroral electrojet over the VLF paths, the LWPC two-dimensional VLF propagation model [*Ferguson and Snyder*, 1987] was employed. This model incorporates realistic values of ground conductivity, ionospheric electron density, and ionospheric electron-neutral collision frequency over the great circle propagation path. Details of the modeling are discussed in section 3.

Armed with these predicted signatures, we examined the magnetometer and VLF data over 17 nighttime periods for which we had complete data sets (January 4-6 and 23-31, 1993; February 23-26 and 28, 1993) for evidence of simultaneous signatures. The results were

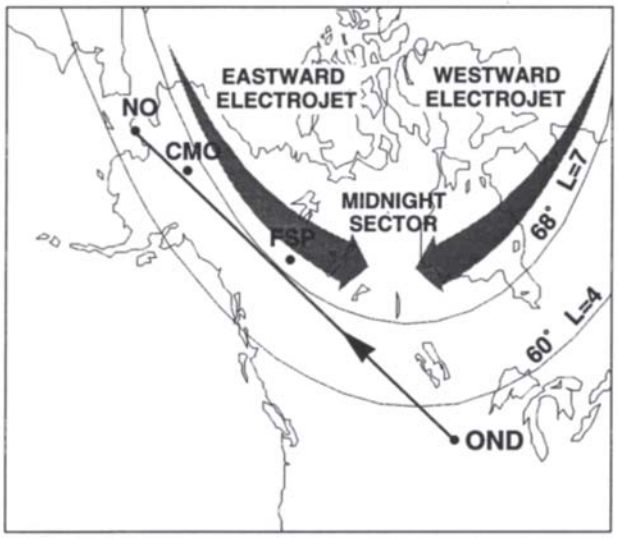

Figure 2. Geographic configuration of VLF transmitter, VLF receiver, and magnetometer stations used in this study. The signal from the Omega North Dakota VLF transmitter (OND, 13.1 kHz, La Moure, North Dakota) was monitored with a receiver in Nome, Alaska (NO). The dark line indicates the VLF great-circle propagation path from the transmitter to the receiver. Magnetometer data from stations in College, Alaska (CMO) and Fort Simpson, Northwest Territories (FSP) were also used. Also shown are the footprints at 100 km altitude of the L=7 (MLAT=68°) and L=4 (MLAT=60°) field lines, nominally representing the position of the equatorward edge of the electrojet during magnetically quiet and disturbed times, respectively.

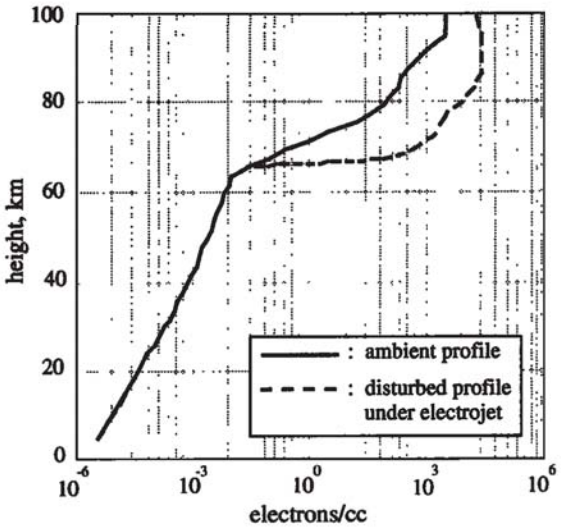

Figure 3. The two electron density profiles used in our simulation. The solid curve is typical of an ambient nighttime density profile, and the dashed curve is the assumed density profile under the electrojet-associated electron precipitation. This latter profile has been calculated from the precipitating electron flux and electron energy spectrum reported by *Kikuchi and Evans* [1983] using the ion-pair production model of *Rees* [1963] and *D* region chemistry model of *Glukhov et al.* [1992].

summarized briefly in section 1, and section 4 contains further statistics and analysis as well as figures showing the actual data from representative nights.

Additionally, during one of the time periods examined, the Freja satellite passed over the area of interest at the same time as the electrojet was starting to cross over the OND-NO path. An analysis of the Freja magnetic field data provides another independent measurement of the southern edge of the electrojet by measuring the position of the region 2 field-aligned currents. This additional independent measure of electrojet position is shown to be consistent with that obtained from the VLF data, further strengthening the VLF-electrojet connection.

3. Simulation Results

As the VLF propagation model is two-dimensional in nature (i.e., no variations transverse to the propagation path), the incursion of the electrojet over each propagation path is modeled as a segment of the Earth-ionosphere waveguide with a perturbed electron density profile caused by the intense electron precipitation. As the electrojet moves southward, more of the path is under the disturbed region of the ionosphere, and we model this motion by increasing the length of the perturbed waveguide segment. Figure 3 shows the ambient and perturbed electron density profiles used for the simulation. The perturbed profile was calculated using the ion-pair production model of *Rees* [1963], the *D* region chemistry model of *Glukhov et al.* [1992], and the precipitating electron flux and electron energy spectrum measured on NOAA 6 during electrojet crossings and reported by *Kikuchi and Evans* [1983].

Figure 4 shows the simulated VLF amplitude and phase variations (on a linear scale) as a function of the extent of the electrojet incursion over the propagation path. As the electrojet expands southward, as

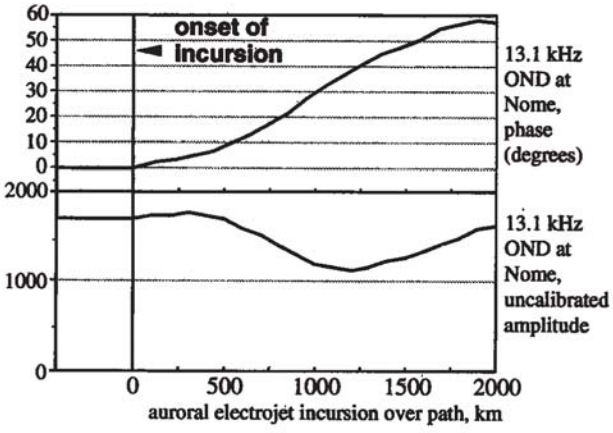

Figure 4. Simulated VLF linear amplitude and phase versus the length of the electrojet incursion over the VLF great circle path. These are the amplitude and phase signatures that are expected at each receiver when the electrojet crosses each propagation path.

it would during a substorm event, the length of the incursion is an approximate measure of time. Thus the VLF amplitude and phase variations plotted in Figure 4 correspond to the temporal variations we expect to observe as the electrojet crosses over the propagation paths shown in Figure 2.

4. Simultaneous VLF and Ground Magnetometer Data

4.1. Summary

As mentioned above, a total of 17 nights of complete VLF and magnetometer data were examined in this study. The complete period examined each night was from 0300 to 1200 UT (for reference, local midnight in College is 0950 UT and in Fort Simpson is 0810 UT). Of these 17 nights, four of them produced quiet magnetometer data from 0300 to 1000 UT at both the CMO and FSP stations. Although some of these nights did show activity after 1000 UT, we officially designated these nights "quiet" due to the extended period without significant magnetometer activity. The simultaneous VLF amplitude and phase data for these four quiet nights showed a similar lack of significant activity. It should be noted that there was an exact one-to-one correspondence between the quiet magnetometer nights and the quiet VLF nights; on any night when one of the data sets showed an event between 0300 and 1000 UT, the other did as well. Data from a representative quiet night (January 23, 1993) are shown in Figure 5. The VLF amplitude data on this night do show a notable amplitude decrease commencing at 0700 UT that is similar to the model predictions, and the VLF data from the other three quiet nights do show some amplitude decreases and some phase advances, but never simultaneously. On the nonquiet nights, we found that each of the VLF signatures correlated with magnetometer activity contain both an amplitude decrease and a phase advance. Therefore we require a simultaneous VLF amplitude decrease and phase advance to denote a VLF event.

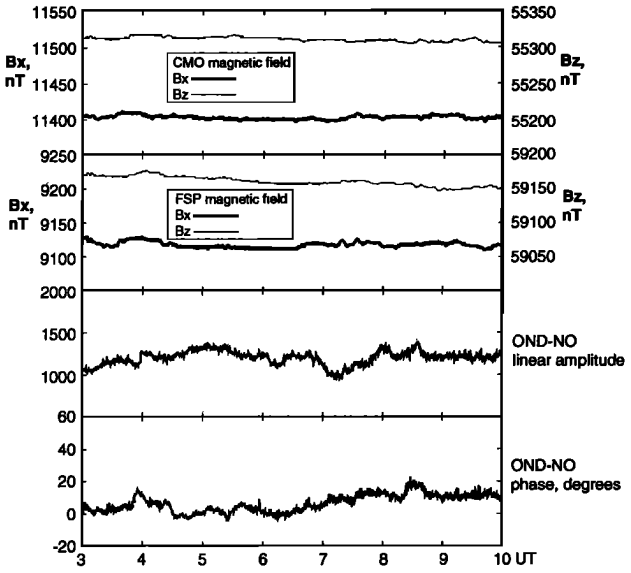

Figure 5. Shown is the magnetometer (B_X and B_Z) and VLF (amplitude and phase) data from 0300-1000 UT for a representative quiet night (January 23,1993). The magnetometer data are totally quiet, and the VLF data show no combined amplitude and phase signatures that are indicative of electrojet activity over the OND-NO path.

Table 1. Classification of Nights Based on Characteristics of VLF and Magnetometer Data

Classification	Number of Nights
Total nights in study	17
Nights quiet from 0300-1000 UT	4
Good time correlation and good match to simulations	5
Good time correlation and poor match to simulations	3
Poor time correlation	5

This leaves 13 nights of observations when there was significant activity in both the magnetometer and VLF data. These nights can be subdivided into three groups, based on both how well-correlated in time the event onsets are from the two main data sets and on how well the observed VLF signatures match the simulations shown in section 3. For five of the nights, we found excellent temporal correlation between VLF events and magnetometer events and good agreement between the observed and simulated VLF amplitude and phase signatures. For three of the nights, we found good temporal correlation between VLF events and magnetometer events but minimal similarity between the observed and simulated VLF signatures. For the remaining five nights, the temporal correlation of magnetometer events and VLF events was rather poor. These results are summarized in Table 1.

4.2. Examples

We now show some representative nights of data from the different classifications shown in Table 1. Figures 6-8 show simultaneous magnetometer and VLF data from February 23, 1993, January 30, 1993, and February 26, 1993, all of which showed good time correlation between the VLF and magnetometer events and had good agreement between the theoretical and observed VLF signatures. On February 23, 1993, an OND amplitude decrease and phase advance commence simultaneously at 0925 UT, and the maximum amplitude decrease and phase advance (which occur simultaneously at 0955 UT) of 40% and 40°, respectively, agree well quantitatively with the simulations. The exact onset of the magnetometer events is difficult to ascertain, but both the CMO and FSP data show the onset of a significant electrojet expansion around 0915 UT. The FSP data do

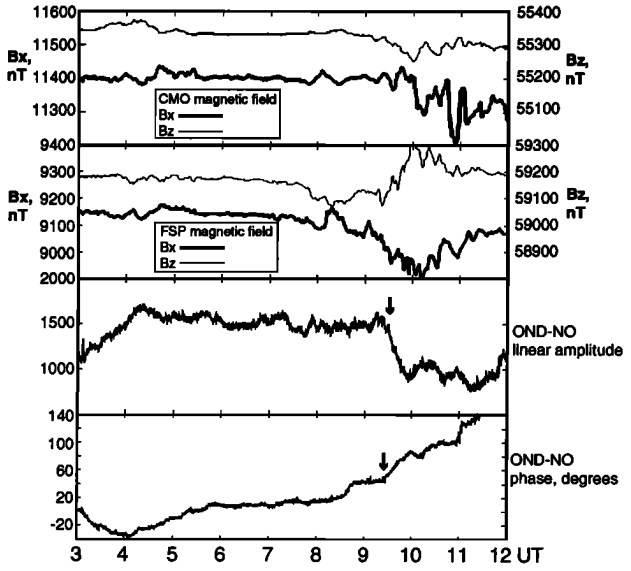

Figure 6. Simultaneous VLF and ground magnetometer data from February 23, 1993. Arrows mark the onset of VLF events. This night exhibited good correlation between the two data sets and a good match of the VLF data to the simulated data shown in Figure 4.

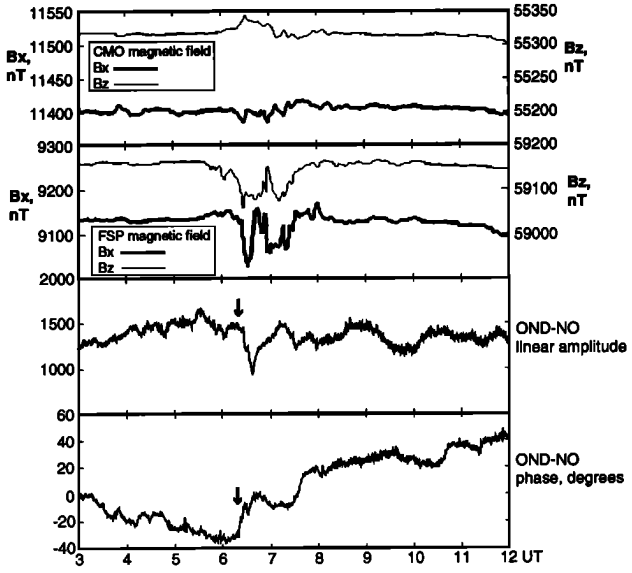

Figure 8. Simultaneous VLF and ground magnetometer data from February 26, 1993. Arrows mark the onset of VLF events. This night exhibited good correlation between the two data sets and a good match of the VLF data to the simulated data shown in Figure 4.

show some small activity as early as 0800 UT, but this is fairly minor and does not indicate that the electrojet had come near the VLF path.

The January 30 data show two distinct VLF events occurring at 0415 and 0825 UT. The first event concerns the premidnight eastward electrojet. The FSP and CMO magnetometer data show event onsets at 0405 and 0425 UT, respectively. This progression is expected for a north to south electrojet expansion, for as seen in Figure 2, the FSP station is farthest north (geomagnetically), in the middle is the OND-NO path, and southernmost is the CMO station. This particular event has a more substantial VLF amplitude decrease relative to the magnitude of the phase advance when compared to the simulations, indicating perhaps a different perturbed electron density profile. The relatively small magnitude of the magnetometer perturbations (compared to the events on other days) for this 0405 UT event also suggest that the event is different from the typical electrojet expansion seen in this data set. The VLF event at 0825 UT is a better match to the model, exhibiting at maximum 30% amplitude drop with a 30° phase advance. The CMO magnetometer data show an electrojet event onset at 0930 UT, and the FSP data, though a bit noisy and difficult to interpret, show electrojet activity beginning at approximately 0800 UT. These data are consistent with the plausible physical picture of the westward electrojet moving slowly southward, crossing FSP at 0800 UT, crossing the OND-NO path at 0830 UT, then temporarily stopping its southward motion and rotating with local midnight to appear over the CMO station at 0930 UT.

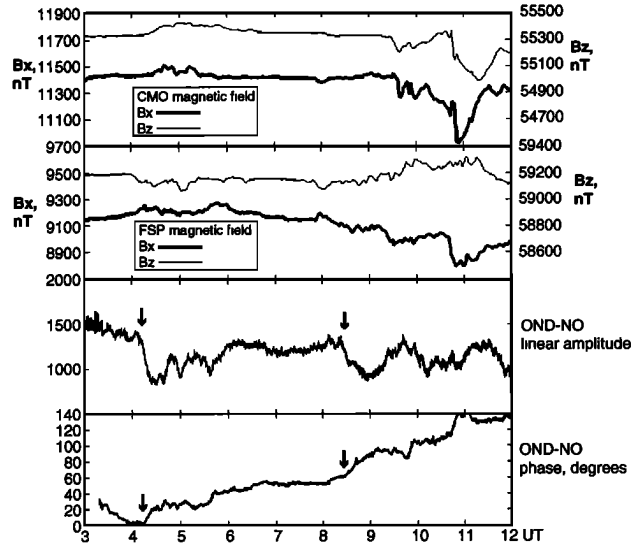

Figure 7. Simultaneous VLF and ground magnetometer data from January 30, 1993. Arrows mark the onset of VLF events. This night exhibited good correlation between the two data sets and a good match of the VLF data to the simulated data shown in Figure 4.

The February 26 data show a VLF amplitude decrease and phase advance onset at 0620 UT. The magnetometer data on this night is particularly interesting, as the FSP data show a sudden electrojet event over the station beginning at about 0610 UT, while the CMO station, 1400 km away, shows no significant activity at all, indicating a very local electrojet expansion. This highlights both the main advantage and disadvantage of VLF-based electrojet monitoring; very local events are captured with a single receiver station, but it is difficult to ascertain where along the path the event oc-

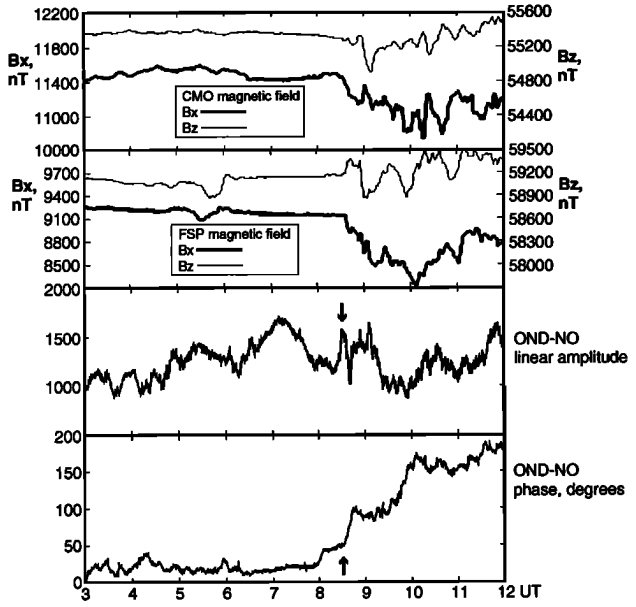

Figure 9. Simultaneous VLF and ground magnetometer data from February 28, 1993. Arrows mark the onset of VLF events. This night exhibited good temporal correlation between the VLF and magnetometer signatures, but the observed VLF data were poor matches to the simulations.

curred without data from additional great circle paths.

A night (February 28, 1993) showing good temporal correlation between the VLF and magnetometer data but a poorer match of the VLF signatures to the model is shown in Figure 9. The magnetometer data are unambiguous on this night; a strong electrojet moved south over both stations nearly simultaneously at 0835 UT, with the center of the electrojet currents passing over FSP at 1005 UT and CMO at 1015 UT (at these times, the perturbation in B_X is a maximum while that in B_Z is zero). The VLF phase data show a rapid (15 min) phase advance of 50° starting at 0832 UT, while the amplitude data show a rapid decrease commencing 0832 UT followed by a equally rapid recovery which begins at 0840 UT when the phase advance is 30°. This VLF signature is different from both the model predictions (Figure 4) and the events shown in Figures 6-8; however, it still meets the VLF event criterion defined earlier and is well-correlated with the magnetometer events. The amplitude increase at 0825 UT comes clearly before the start of the phase advance when viewed with higher time resolution, and for this reason it is not interpreted as part of the electrojet-associated VLF signature.

Data from a night in the poorly correlated group (January 6, 1993) are shown in Figure 10. The data show a number of magnetometer and VLF events, but, in contrast to the nights shown previously, the temporal correlation between them was rather poor. The FSP magnetometer data show three distinct electrojet movements over the station at 0520, 0635, and 1015 UT, and the CMO data show minor activity commencing at 0515, 0700, and 1010 UT. The VLF data show a strong amplitude and phase event at 0455 UT and another at 1015 UT. However, the clearest VLF event, at 0455 UT, occurs 20 min prior to any activity seen in the magnetometer data. One explanation of this time difference is that a very local electrojet event occurred directly between the magnetometer stations (although closer to FSP than to CMO based on the size of the magnetic perturbations), and thus the VLF path was crossed before any measurable perturbations were observed in the magnetometer data.

4.3. Discussion

We have shown a number of cases which exhibit a clear temporal correlation between electrojet signatures seen in ground magnetometer data and simultaneous VLF amplitude decreases and phase advances. In most cases, the agreement between the observed VLF signatures and those predicted with the LWPC model is quite good in terms of magnitude and shape. However, we do not observe the predicted slight amplitude increase at the onset of the event.

A possible explanation for the nights when the VLF observations did not match the model, but the magnetometer/VLF event time correlation was good is revealed in an examination of the 3-hour K_P indices for the period studied. The three nights in this group had the three highest K_P averages over the 12-hour period 0000-1200 UT of all the nights in the study (average $K_P \geq 4$ for these nights), indicating that the geomagnetic activity on these nights was higher than usual. Since these nights were markedly different from the majority in terms of the overall level of geomagnetic activ-

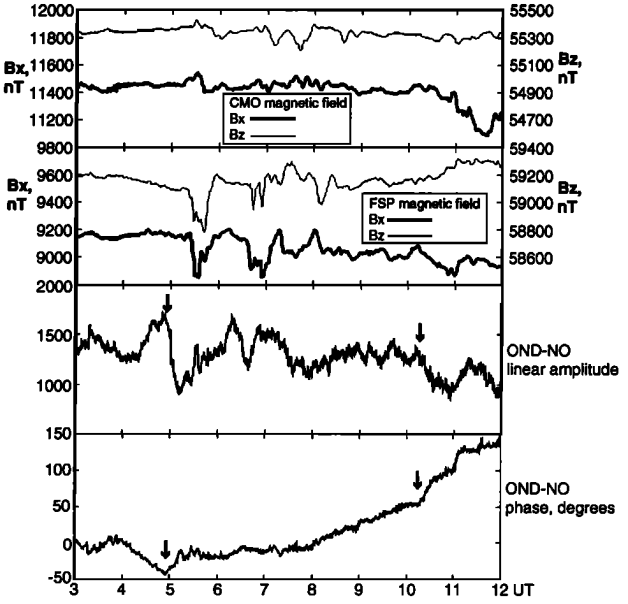

Figure 10. Simultaneous VLF and ground magnetometer data from January 6, 1993. Arrows mark the onset of VLF events. This night exhibited rather poor temporal correlation between the VLF and magnetometer signatures, as the VLF event at 0455 UT precedes any magnetometer activity by 20 min.

ity, it seems likely that the intensity and energy spectrum of the electrojet-associated electron precipitation was also different from the usual, leading to different perturbed electron density profile and a different VLF signature.

The data on the five nights with poor temporal correlation also exhibited broad similarity. These nights tended to show either multiple magnetometer and VLF events (like the night shown in Figure 10) or magnetometer events with very gradual onsets, making it difficult to assign an onset time for the magnetometer event. In both cases, however, the VLF events appeared from 20 min to more than an hour before a magnetometer event. As mentioned above, it is possible that very local electrojet expansions that occur between the magnetometer stations cause the advanced VLF event signature. The data from February 26, 1993 demonstrate that such localized electrojet expansions to occur. We do not believe it is very likely that an entirely unrelated ionospheric disturbance caused a false positive event recognition, for in the four quiet nights in the data set, no VLF events were seen.

5. Freja Magnetometer Data On 23 Feb 1993

Quite serendipitously, on February 23, 1993, the Freja satellite flew over southern Alaska at about 0920 UT, which is exactly the time at which both the VLF and magnetometer data indicated that the electrojet was crossing the area. We can further validate the VLF technique by comparing the estimate of the position of the edge of the electrojet from the space-based measurement and the estimate based on the VLF data. Ground magnetometer data do not readily provide information on the position of the edge, so this measurement is not included in the comparison.

As mentioned above, it has been previously found that the equatorward edge of the electrojet is at the same magnetic latitude as the equatorward edge of the region 2 field-aligned currents flowing in the magnetosphere [*Zanetti et al.*, 1983]. Additionally, *Potemra et al.* [1994] verified the latitudinal association of the electrojet currents and field-aligned currents from simultaneous Freja and UARS measurements. Satellite magnetic field data directly provide the position of these field-aligned currents.

Shown in Figure 11 is Freja magnetic field data from February 23, 1993. This particular pass was over the region of interest at almost exactly the same time for which we have an estimate of the electrojet position based on VLF and ground magnetometer data. The data show a triangular perturbation in the B_E (eastward magnetic field) component between 0919:30 and 0924:45. Perturbations of this nature are usually interpreted as a region 2/region 1 field-aligned current pair, and information concerning the magnitude of the field-aligned currents and associated electrojet currents can be extracted from measurements of this type [*Potemra et al.*, 1994]. As we are mainly concerned with the location of edge of the electrojet, we focus on the eastward turning of the magnetic field seen by Freja at 0919:30 UT, which indicates that the satellite was entering the downward currents comprising the premidnight side region 2 currents. Mapping the Freja geographic location along the magnetic field, we find the footprint at 100 km altitude of the satellite path, and we infer that the low-latitude edge of the auroral electrojet was at 65.5°N geographic latitude at a longitude of -147°E at 0919:30 UT.

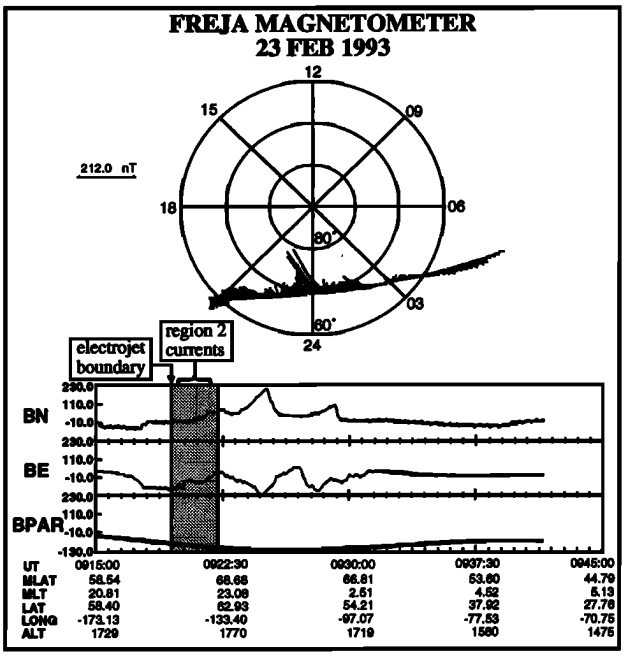

Figure 11. Freja satellite magnetometer data from February 23, 1993 between 0915 and 0945 UT. This particular pass was directly over the VLF-estimated position of the auroral electrojet. The eastward turning of of the magnetic field (positive perturbation in B_E) at 0919:30 UT indicates the satellite began passing through the region 2 field-aligned currents, and therefore passed over the southern edge of the electrojet, at 64.5°N geographic latitude.

We can also derive an estimate of the edge of the electrojet from the VLF data. We know that the edge of the electrojet-associated particle precipitation began to cross over the OND-NO path at 0925 UT. If we assume that the lower edge of the electrojet follows lines of constant geomagnetic latitude, we can deduce the position of the lower edge of the electrojet at 0925 UT.

In Figure 12, we graphically show the information concerning the electrojet position extracted from the VLF and Freja measurements. The Freja flight path is shown by the dashed line, and the cross marks the spot at which it entered the region 2 currents and thus began passing over the electrojet. The VLF-based estimate of the lower edge is shown by the solid line. Note that the VLF estimate is at 0925 UT and the Freja estimate is at 0919:30 UT, so we expect the Freja estimate to be slightly north of the VLF estimate, for both the VLF

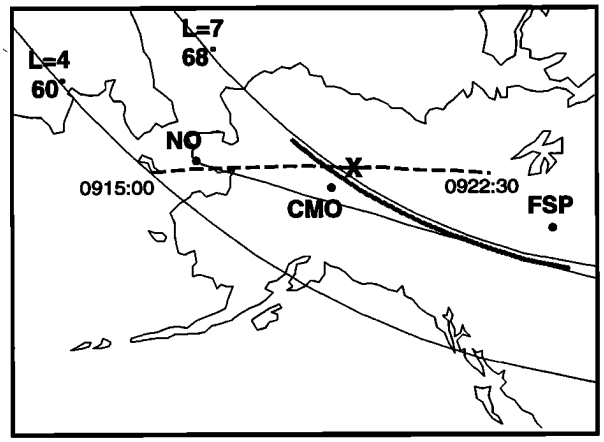

- - - - - : Freja path with times, 23 Feb 1993
X : Edge of electrojet from Freja data, 23 Feb 1993, 0919:30 UT
——— : Edge of electrojet from VLF data, 23 Feb 1993, 0925:00 UT

Figure 12. A geographic view of the measurements of electrojet position on February 23, 1993 based on the VLF amplitude and phase data and the Freja magnetometer data.

slightly north of the VLF estimate, for both the VLF and ground magnetometer data show the electrojet to be moving south during this time period. As can be seen in Figure 12, the two independent measurements are completely consistent.

6. Summary and Conclusions

The possibility of determining the position of the auroral electrojet from measurements of subionospherically propagating VLF signals was examined. Within the auroral zone, precipitating electrons associated with the electrojet with $E > 300$ keV create secondary ionization at altitudes low enough to affect the propagation of the VLF signals underneath. We examined 17 nights of VLF amplitude and phase data and ground magnetometer data, and found that there was excellent time correlation between magnetometer events and VLF events (a VLF event being defined as a simultaneous VLF amplitude drop and phase advance) in eight of the 13 nights that showed electrojet activity in the magnetometer data. Additionally, on five of those eight nights of good time correlation, the observed VLF signatures associated with the auroral electrojet were very similar in form and magnitude to those predicted by the two-dimensional VLF propagation model, indicating an enhanced D region electron density profile close to that in Figure 3. On the three nights when the VLF data did not match the model well but did exhibit good time correlation with the ground magnetometer data, the K_P index was higher than on all other nights in the study, and we suspect that the electron precipitation was also markedly different on these nights, causing the altered form of the VLF signature. We also found five nights on which the VLF/magnetometer correlation was rather poor and inconclusive, and a number of potential causes were discussed.

For one of the nights studied (February 23, 1993), Freja satellite magnetometer data was also available and provided an additional measurement of the electrojet position. We found that the independent measurements of the southern edge of the electrojet from the VLF and Freja data were completely consistent.

We conclude that unique VLF phase and amplitude changes are often associated with the appearance of auroral electrojet activity at magnetometer sites near the VLF propagation path. We interpret this association as being due to the motion of the electrojet over the propagation path. Further tests of this potential electrojet detection technique should be carried out using at least two VLF receiving sites at each of which multiple VLF propagation paths would be monitored. The resultant detailed electrojet mapping could then be compared with similar mappings using magnetometer and spacecraft data in order to provide full proof of concept. The ability to map the auroral electrojet from continuous ground-based measurements would be valuable in the study of substorm phenomena, auroral particle precipitation effects on the lower ionosphere, and the generation mechanisms of atmospheric gravity waves.

References

Baker, D. N., R. A. Goldberg, F. A. Herrero, J. B. Blake, and L. B. Callis, Satellite and rocket studies of relativistic electrons and their influence on the middle atmosphere, *J. Atmos. Terr. Phys., 55*, 1619, 1993.

Burgess, W.C., and U. S. Inan, The role of ducted whistlers in the precipitation loss and equilibrium flux of radiation belt electrons, *J. Geophys. Res., 98*, 15,643, 1993.

Callis, L. B., D. N. Baker, J. B. Blake, J. D. Lambeth, R. E. Boughner, M. Natarajan, R. W. Klebesadel, and D. J. Gorney, Precipitating relativistic electrons: Their long-term effect on stratospheric odd nitrogen levels, *J. Geophys. Res., 96*, 2939, 1991.

Chenette, D. L., D. W. Datlowe, R. M. Robinson, T. L. Schumaker, R. R. Vondrak, and J. D. Winningham, Atmospheric energy input and ionization by energetic electrons during the geomagnetic storm of 8-9 November 1991, *Geophys. Res. Lett., 20*, 1323, 1993.

Ferguson, J. A., and F. P. Snyder, The segmented waveguide program for long wavelength propagation calculations, *Tech. Doc. 1071*, Nav. Ocean Sys. Cent., San Diego, Calif., 1987.

Francis, S. H., A theory of medium-scale traveling ionospheric disturbances, *J. Geophys. Res., 79*, 5245, 1974.

Glukhov, V. S., V. P. Pasko, and U. S. Inan, Relaxation of transient lower ionospheric disturbances caused by lightning-whistler-induced electron precipitation bursts, *J. Geophys. Res., 97*, 16971, 1992.

Hunsucker, R. D., Atmospheric gravity waves generated in the high-latitude ionosphere: A review, *Rev. Geophys., 20*, 293, 1982.

Inan, U. S., F. A. Knifsend, and J. Oh, Subionospheric VLF "imaging" of lightning-induced electron precipitation from the magnetosphere, *J. Geophys. Res., 95*, 17217, 1990.

Kamide, Y. R., S. I. Akasofu, B. H. Ahn, W. Baumjohann,

and J. L. Kisabeth, Total current of the auroral electrojet estimated from the IMS Alaska Meridian chain of magnetic observatories, *Planet. Space Sci., 130*, 621, 1982.

Kikuchi, T., and D. S. Evans, Quantitative study of substorm-associated VLF phase anomalies and precipitating energetic electrons on November 13, 1979, *J. Geophys. Res., 88*, 871, 1983.

Potemra, T. A., L. J. Zanetti, B. J. Anderson, P. F. Bythrow, and S. Ohtani, Freja's contribution to the ISTP Event of October 27, 1992: A distorted magnetosphere, *Geophys. Res. Lett., 21*, 1871, 1994.

Potemra, T. A., and T. J. Rosenberg, VLF propagation disturbances and electron precipitation at mid-latitudes, *J. Geophys. Res., 78*, 1572, 1973.

Rees, M. H., Auroral ionization and excitation by incident energetic electrons, *Planet. Space Sci., 11*, 1209, 1963.

Ringlee, R. J., Geomagnetic effects on power systems, *IEEE Power Eng. Rev., 9*, 6, 1989.

Yeh, K. C., and C. H. Liu, Acoustic-gravity waves in the upper atmosphere, *Rev. Geophys., 12*, 193, 1974.

Zanetti, L. J., W. Baumjohann, and T. A. Potemra, Ionospheric and Birkeland current distributions inferred from the MAGSAT magnetometer data, *J. Geophys. Res., 88*, 4875, 1983.

T. F. Bell, S. A. Cummer, and U. S. Inan, Space, Telecommunications and Radioscience Laboratory, Stanford University, Stanford, CA 94305.

L. J. Zanetti, Applied Physics Laboratory, Johns Hopkins University, Laurel, MD 20723.

(Received March 1, 1995; revised October 19, 1995; accepted October 31, 1995.)